British Journal of Cancer (2012) 107, 739 – 747

www.bjcancer.com

Lipoprotein lipase is frequently overexpressed or translocated in cervical squamous cell carcinoma and promotes invasiveness through the non-catalytic C terminus

SA Carter[1,2], NA Foster[2], CG Scarpini[1,2], A Chattopadhyay[2], MR Pett[1,2], I Roberts[2] and N Coleman*[,1,2]

[1]Department of Pathology, University of Cambridge, Tennis Court Road, Cambridge CB2 1QP, UK; [2]Medical Research Council Cancer Cell Unit, Hutchison-MRC Research Centre, Cambridge CB2 0XZ, UK

BACKGROUND: We studied the biological significance of genes involved in a novel t(8;12)(p21.3;p13.31) reciprocal translocation identified in cervical squamous cell carcinoma (SCC) cells.

METHODS: The rearranged genes were identified by breakpoint mapping, long-range PCR and sequencing. We investigated gene expression *in vivo* using reverse-transcription PCR and tissue microarrays, and studied the phenotypic consequences of forced gene overexpression.

RESULTS: The rearrangement involved *lipoprotein lipase* (*LPL*) and *peroxisome biogenesis factor-5* (*PEX5*). Whereas *LPL–PEX5* was expressed at low levels and contained a premature stop codon, *PEX5–LPL* was highly expressed and encoded a full-length chimeric protein (including the majority of the *LPL* coding region). Consistent with these findings, *PEX5* was constitutively expressed in normal cervical squamous cells, whereas *LPL* expression was negligible. The *LPL* gene was rearranged in 1 out of 151 cervical SCCs, whereas wild-type *LPL* overexpression was common, being detected in 10 out of 28 tissue samples and 4 out of 10 cell lines. Forced overexpression of wild-type *LPL* and *PEX5–LPL* fusion transcripts resulted in increased invasiveness in cervical SCC cells, attributable to the C-terminal non-catalytic domain of LPL, which was retained in the fusion transcripts.

CONCLUSION: This is the first demonstration of an expressed fusion gene in cervical SCC. Overexpressed wild-type or translocated *LPL* is a candidate for targeted therapy.

British Journal of Cancer (2012) **107,** 739–747. doi:10.1038/bjc.2012.301 www.bjcancer.com
Published online 10 July 2012

Keywords: lipoprotein lipase; cervix; carcinoma; invasion; chromosome translocation; peroxisome biogenesis factor-5

Cervical carcinoma is the third most common cause of cancer deaths in women worldwide, with approximately 500 000 new cases and 300 000 deaths per annum (Baldwin *et al*, 2003). Eighty percent of cases are squamous cell carcinomas (SCCs), which arise in a multistep fashion from precursor squamous intra-epithelial lesions (Arends *et al*, 1998; Holowaty *et al*, 1999; Pett and Coleman, 2007). Unlike most other malignancies, cervical carcinoma has a single causative agent, high-risk human papillomavirus (HR-HPV; Bosch *et al*, 1995; Walboomers *et al*, 1999). However, HR-HPV infection is insufficient for malignant progression, with host genomic instability also thought to be required (zur Hausen, 2000). Chromosomal instability is the most common form of genomic instability in cervical cancer, with malignant progression being associated with increasing levels of both structural and numerical chromosomal abnormalities (Heselmeyer *et al*, 1996; Harris *et al*, 2003; Rao *et al*, 2004; Hidalgo *et al*, 2005; Lockwood *et al*, 2007).

The specific host chromosomal abnormalities that drive progression of cervical SCC remain poorly understood. It is likely that these include gene fusions caused by chromosomal translocations, which are increasingly being recognised as important in solid tumours (Tomlins *et al*, 2005; Soda *et al*, 2007; Edwards, 2010). We previously undertook a systematic molecular cytogenetic analysis of cervical SCC cells to identify potential driver genes in cervical carcinogenesis (Foster *et al*, 2009). The work revealed a novel reciprocal translocation t(8;12)(p21;p12), which was present in 100% of metaphases of the cell line MS751. This cell line is hypo-tetraploid, presumably having undergone endoreduplication followed by chromosome loss (Ganem *et al*, 2007). The translocation was duplicated in all cells, indicating that it occurred before endoreduplication. In addition, at least one derivative chromosome formed by the translocation was present in independent karyotypic analyses of MS751 cells (Dowen *et al*, 2003; Harris *et al*, 2003). Together, these findings indicated that the t(8;12) translocation was either present in the tumour from which MS751 was derived, or was acquired early in the establishment of the cell line *in vitro*. Abnormalities in the latter category may also be of significance in cervical carcinogenesis, as chromosomal abnormalities that develop in HR-HPV-infected cell lines *in vitro* often reflect those seen in clinical samples, presumably because similar selective pressures apply *in vivo* and *in vitro* (Pett *et al*, 2004).

In view of these observations, we sought to identify whether the t(8;12) translocation in MS751 involved gene(s) of broad functional significance in cervical carcinogenesis. This approach was justified, as recurrent fusions of importance in cancer, such as *ELM4–ALK*, were previously identified following investigation of

*Correspondence: Professor N Coleman; E-mail: nc109@cam.ac.uk
Received 3 May 2012; accepted 13 June 2012; published online 10 July 2012

individual cases (Soda *et al*, 2007). We demonstrated two novel fusion genes that were produced by the translocation in MS751, one of which, *peroxisome biogenesis factor-5–lipoprotein lipase* (*PEX5–LPL*), led to the identification of *LPL* as a recurrently overexpressed potential oncogene in cervical SCC.

MATERIALS AND METHODS

Cervical SCC cell lines and tissue samples

The cervical SCC cell lines studied were the following: C33A, C-4I, C-4II, CaSki, DoTc2, HT-3, ME180, MS751, SiHa and SW756. Full details are given elsewhere (Ng *et al*, 2007). All cells were obtained from the American Type Culture Collection and grown in Glasgow minimum essential medium, 10% fetal calf serum (FCS), 1 U ml^{-1} penicillin and 1 μg ml^{-1} streptomycin. The FCS was a source of lipoproteins in functional studies of the cell lines.

All tissue samples were anonymised and used with approval from the relevant Local Research Ethics Committees. The samples used were: (i) normal cervical squamous epithelium microdissected from 5 hysterectomy specimens removed for non-neoplastic disease unrelated to the cervix and (ii) 28 primary cervical SCCs obtained from the archives of the Kidwai Memorial Institute of Oncology, Bangalore, India (Ng *et al*, 2007). In addition, we used three tissue microarrays (TMAs), namely CXC1501 and CXC1021 (Pantomics, Richmond, CA, USA), and CR803 (Biomax, Rockville, MD, USA). Together, these contained 12 separate normal cervical epithelium samples and 151 separate primary cervical SCCs.

Fluorescence *in situ* hybridisation

Bacterial artificial chromosome (BAC) and fosmid clones were obtained from BACPAC Resources (Oakland, CA, USA; Supplementary Tables S1 and S2), and DNA extracted as described previously (Shing *et al*, 2003). Whole-chromosome-specific probes were generated by amplifying flow-sorted chromosomes, using degenerate oligonucleotide-primed PCR and labelling directly with Spectrum Orange dUTP (Vysis, Downers Grove, IL, USA). The BAC and fosmid probes were labelled by nick translation (Vysis) with either digoxigenin 11-dUTP or biotin 16-dUTP (Roche, Basel, Switzerland). Avidin-Cy3 or -Cy5 (1 : 400; Amersham, Little Chalfont, UK) and biotin anti-avidin (1 : 300) were used to detect biotin-labelled probes, whereas anti-digoxigenin FITC (1 : 500; Boehringer Mannheim, Mannheim, Germany), rabbit anti-FITC (1 : 300) and goat anti-rabbit-FITC were used to detect digoxigenin-labelled probes.

Metaphase BAC fluorescence *in situ* hybridisation (FISH) was performed as described previously (Ng *et al*, 2007). For fibre FISH, DNA fibres were prepared by lysing cells in 75 mM KCl (20 min, 37 °C) and fixing in 3 : 1 methanol : acetic acid. The cell suspension was spread horizontally across a glass slide, which was immediately immersed in lysis buffer (0.5% (w/v) SDS, 50 mM EDTA, 0.2 M Tris-HCl (pH 7.4); 5 min) in a Coplin jar. Ethanol (94%) was added dropwise above the lysis buffer, and slides incubated for 10 min to precipitate DNA at the solution interface. Slides were removed from the Coplin jar slowly at an angle to spread DNA fibres along the slide, incubated in 70% ethanol (30 min) to fix fibres to the slide, and dehydrated through an ethanol series before air drying and storing at 37 °C. Probes (prepared as for metaphase BAC FISH) were denatured for 10 min at 72 °C and pre-annealed at 37 °C for 30–60 min. Fibre slides were prepared by incubating (3 min each) in denaturation solution (0.5 M NaOH, 1.5 M NaCl), neutralisation solution (0.5 M Tris-HCl, 3 M NaCl) and 2 × standard saline citrate, before dehydrating through an ethanol series, air drying and storing at 37 °C. Hybridisation of the probe to the DNA fibres was performed at 37 °C in a dark humidified box for 24 h. Post-hybridisation washes and detection were performed as for metaphase BAC FISH. Fluorescent *in situ* hybridisation on TMAs was performed as described previously (Shing *et al*, 2003).

Images were captured with an Axioplan II fluorescence microscope (Zeiss, Welwyn Garden City, UK) equipped with a charge-coupled device camera (Applied Spectral Imaging, Carlsbad, CA, USA), controlled by SmartCapture software (Vysis). For metaphase and fibre FISH, at least 10 images were captured. For each TMA, 5 images were taken across each core, and 60 SCC cell nuclei scored for each case. The interpretation of intact and split signals was based on generally accepted guidelines recommended by Vysis and used for break-apart FISH assays in clinical laboratories. This approach requires the space between two signals to be greater than one signal width, to be considered a split signal (Patel *et al*, 2005).

Long-range PCR

Genomic DNA was extracted as described previously (Shing *et al*, 2003). Long-range PCR was used to amplify across the breakpoints of der(8) (primers 5′-TTCACCCAGGACAAGGCCCTT-3′ and 5′-GGTGAATGTGTGTAAGACGTC-3′) and der(12) (primers 5′-GCCCACCTGTATCTTTCACATC-3′ and 5′-CACTCTGTTACTTTTGTCTCCTTC-3′), using Platinum PCR SuperMix High Fidelity (Invitrogen, New York, NY, USA). Products were then sequenced, either directly following gel electrophoresis or following cloning into TOPO vectors (Invitrogen).

Reverse-transcription PCR

RNA was extracted from cell lines or tissue samples and reverse transcribed as described previously (Ng *et al*, 2007). The cDNA templates were amplified by PCR, to allow qualitative detection of *LPL* and *PEX5* transcripts. We used AmpliTaq Gold DNA polymerase (Applied Biosystems, Foster City, CA, USA) and the primers described in Supplementary Table S3. Products were cloned into TOPO vectors before sequencing.

Quantitative reverse-transcription PCR (qRT–PCR) was performed as described previously (Ng *et al*, 2007), using primers listed in Supplementary Table S4. Expression ratios of test samples relative to reference were calculated using the comparative C_t method (Pfaffl, 2001), normalising to four different housekeeping genes. Ratios were referenced to Universal Reference cDNA (Stratagene, Santa Clara, CA, USA), which was derived from a broad range of cell types, including those with abundant *LPL* expression (e.g., liver cells). A cervical SCC sample was defined as showing overexpression of *LPL* if the mean expression level (calculated using the four housekeeping genes) was greater than three s.d. above the mean of the five normal cervix samples.

Generation of stable cell lines expressing wild-type LPL or fusion genes

LPL, *PEX5–LPL* and *PEX5–LPLvar* cDNA were cloned into pcDNA3.1/zeo(+) (Invitrogen) and transfected into SW756 cells with Lipofectamine 2000 (Invitrogen), 48 h after seeding in OptiMEM-I (Invitrogen). In parallel experiments, vector-only cells were generated to act as negative controls. Stably transfected cells were selected in 100 μg ml^{-1} Zeocin for 3–5 weeks, and stable colonies pooled. In addition, *LPL* cDNA was cloned into pcDNA4/myc-His (Invitrogen) and stably transfected into C33A cells. In the absence of satisfactory antibodies (data not shown), expression levels of all transgenes were assessed by qRT–PCR, using primers specific to the C terminus of *LPL* (Supplementary Table S4).

Cell phenotype assays

To assess cell proliferation rates, 1.4×10^4 stably transfected cells were seeded in 24-well plates, and cell numbers measured at 24-h intervals for 10 days, using a Countess Automated Cell Counter (Invitrogen). All experiments were performed in triplicate.

The average growth rate for each cell line was determined over the 24-h periods showing greatest exponential growth.

Cell invasion assays were performed using a Cultrex Basement Membrane Extract Cell Invasion Assay (Trevigen, Gaithersberg, MD, USA) according to the manufacturer's directions. Cells that had invaded were quantified using Calcein-AM, which is internalised and cleaved to generate fluorescent free Calcein. Standard curves were performed for each control and transgene-expressing cell line, to allow conversion of fluorescence values into cell numbers. All assays were performed in triplicate.

RESULTS

Mapping reciprocal translocation breakpoints in MS751 identified two novel fusion genes

Initial karyotyping using chromosome painting placed the breakpoints of the MS751 reciprocal translocation at 8p21 and 12p12 (Foster *et al*, 2009). We extended this work by mapping the breakpoints to nucleotide level, by sequentially performing BAC FISH on metaphase spreads, fosmid FISH on DNA fibres and long-range PCR spanning the breakpoints.

We first hybridised BACs (approximately 150 kb in length) mapping to 1-Mb intervals around the suspected breakpoints, to metaphases of MS751. This allowed the breakpoint localisation to be refined to 1-Mb regions in chromosome bands 8p21.3 and 12p13.31 (data not shown). Next, BACs tiling each 1-Mb region were hybridised to MS751 metaphases, along with whole chromosome paint for the translocation partner chromosome (i.e., chromosome 12 for the 8p probes and chromosome 8 for the 12p probes). Such co-hybridisation enabled the derivative chromosomes resulting from the reciprocal translocation, der(8) and der(12), to be distinguished from each other, and from normal chromosomes 8 and 12. This resolved the breakpoints to 150 kb for chromosome 8 (the region covered by BAC RP11-70F13, which split and hybridised to both derivatives; Figure 1A) and 95 kb for chromosome 12 (the overlapping region covered by BACs RP11-273B20 and RP11-653C9, which both split; Figure 1B). We identified two genes at the centre of these regions, namely *LPL* (encoding lipoprotein lipase) on chromosome 8 and *PEX5* (encoding peroxisomal biogenesis factor 5) on chromosome 12 (Figure 1A and B). Both genes were on the forward DNA strand.

To increase further the resolution of breakpoint mapping, we used DNA fibres of MS751. These were hybridised with fosmids (approximately 40 kb in length) tiling the target regions, beginning with those spanning the genes of interest. The fosmids were co-hybridised with two other probes mapping to the translocation partner chromosome. The first was a BAC (labelled blue) that hybridised to the breakpoint on the translocation partner. Splitting of this BAC allowed the derivative chromosomes to be distinguished from normal chromosomes and also suggested the distance of the fosmid from the relevant breakpoint. The second co-hybridised probe was a marker BAC (labelled red) for the translocation partner, which mapped centromeric to the breakpoint. These BACs enabled the der(8) and der(12) to be distinguished (Figure 2A).

Of the chromosome 8 fosmids used, D11 (Figure 2B) was only found on der(12) (labelled with the chromosome 12 marker BAC), whereas H10 (Figure 2B) was only found on der(8) (labelled with the splitting chromosome 12 BAC, but not with the marker chromosome 12 BAC). These findings implied that the chromosome 8 breakpoint was between the sequences to which fosmids D11 and H10 mapped (Figure 2A). As the sequences overlapped,

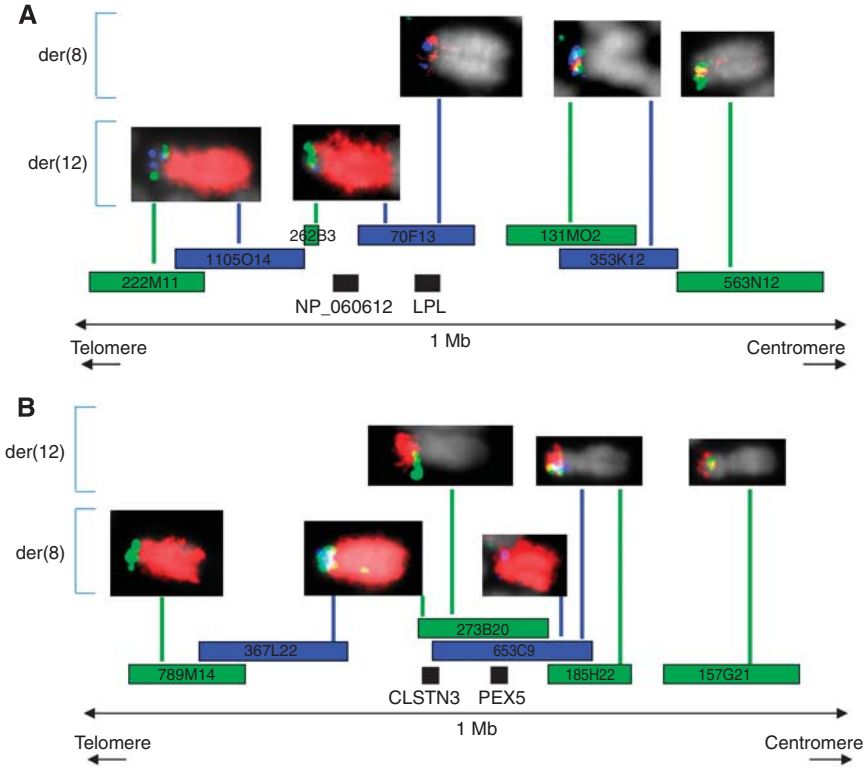

Figure 1 Breakpoint mapping by metaphase BAC FISH. The panels show hybridisation to der(8) and der(12) in MS751 metaphase spreads of BAC probes (labelled blue or green) that mapped to the selected 1-Mb regions on 8p21.3 (**A**) and 12p13.31 (**B**). For each probe, the reciprocal chromosome in the translocation (i.e., chromosome 12 in (**A**) and chromosome 8 in (**B**)) was labelled in red. Where a BAC did not hybridise to a derivative chromosome, the image is not shown. The BACs that hybridised to both der(8) and der(12) (i.e., 'splitting' BACs) were the chromosome 8 BAC RP11-70F13 (**A**) and the chromosome 12 BACs RP11-273B20 and RP11-653C9 (**B**).

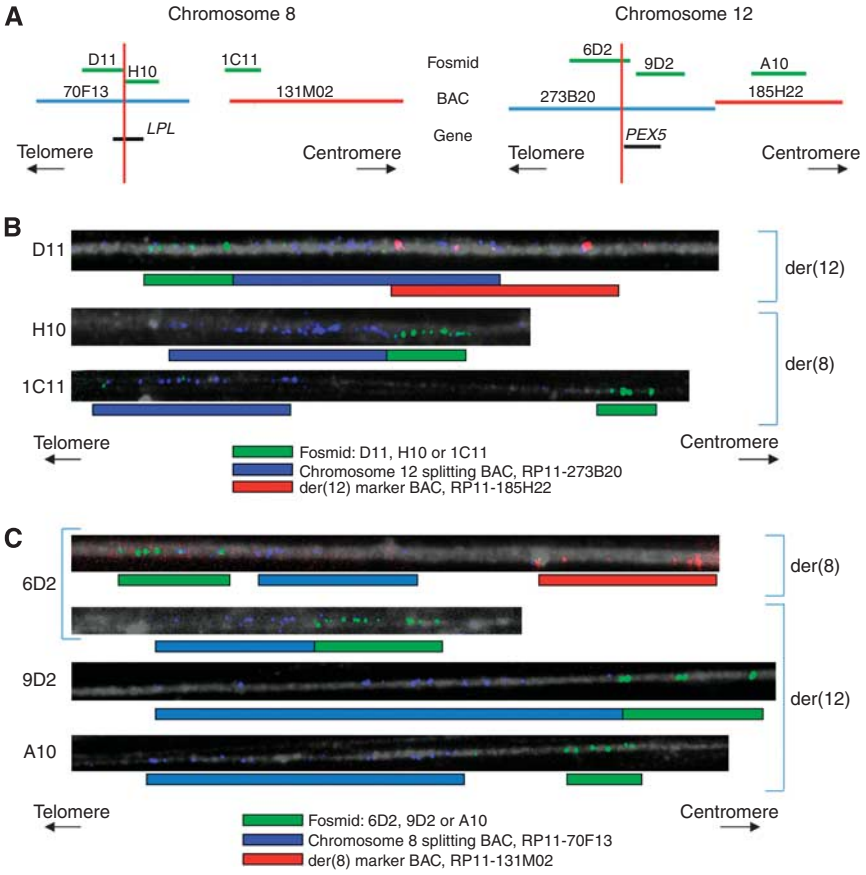

Figure 2 Breakpoint mapping by fosmid fibre FISH. (**A**) The fosmid probes (labelled green) selected for hybridisation to MS751 chromosome fibres either tiled the genes of interest on chromosome 8 and 12 (*LPL* and *PEX5*) or were located centromeric to the breakpoint region, and therefore acted as a control. The fosmids were co-hybridised with BAC probes that mapped to the breakpoint of the reciprocal chromosome (labelled blue) or centromeric to it (labelled red). (**B**) Of the chromosome 8 fosmids, D11 hybridised to der(12) (co-localisation of green signals with both blue and red signals), whereas H10 and 1C11 hybridised to der(8) (co-localisation of green signals with only blue signals). (**C**) Of the chromosome 12 fosmids, 6D2 split between der(8) and der(12) (co-localisation of green signals with both blue and red signals on some fibres, and with blue signals alone on other fibres), whereas 9D2 and A10 hybridised to der(12) (co-localisation of green signals with only blue signals). The suspected breakpoint regions on each chromosome determined by fosmid fibre FISH are shown in panel (**A**) (red vertical lines).

we concluded that the chromosome 8 breakpoint was very close to the centromeric end of D11 or the telomeric end of H10, with the region of each fosmid that hybridised to the opposite derivative chromosome being so small that it was undetectable by FISH. This positioned the breakpoint within the *LPL* coding sequence (Figure 2A).

Of the chromosome 12 fosmids used, 6D2 (Figure 2C) hybridised to both der(8) (labelled with the chromosome 8 marker BAC) and der(12) (labelled with the splitting chromosome 8 BAC, but not with the chromosome 8 marker BAC). This indicated that the chromosome 12 breakpoint was within the sequence to which the 6D2 fosmid mapped. In addition, the chromosome 12 fosmid 9D2 (Figure 2C) hybridised very close to the site of hybridisation of the splitting chromosome 8 BAC on der(12). This suggested that the 9D2 sequence was also in close proximity to the breakpoint, positioning the breakpoint towards the centromeric end of the sequence that fosmid 6D2 mapped to. This implied that the chromosome 12 breakpoint was very close to the 5′-end of the *PEX5* coding sequence (Figure 2A).

Next, 15-kb regions were selected around the suspected breakpoints on each chromosome, and long-range PCR performed using primers in these regions (for primer sequences, see Materials and Methods). We sought to amplify across the breakpoints on der(8) and der(12) to obtain DNA for sequencing. This work revealed that, for der(12), the breakpoints were within intron 3–4 of *LPL* and one base into exon 2 of *PEX5* (Figure 3A). For der(8), the breakpoints were in introns 1–2 of *PEX5* (17 bases more telomeric than the breakpoint in der(12)) and in intron 3–4 of *LPL* (11 bases more telomeric than the breakpoint in der(12); Figure 3B). Therefore, the reciprocal t(8;12)(p21;p13) translocation in MS751 created two novel fusion genes, *PEX5–LPL* on der(8) and *LPL–PEX5* on der(12).

PEX5–LPL was expressed at higher levels from the *PEX5* promoter

We used RT–PCR to show that both fusion genes were transcribed in MS751 (Figure 4A). Sequencing the *LPL–PEX5* PCR product demonstrated that splicing occurred from the 3′-end of *LPL* exon 3 into *LPL* intron 3–4, just before the *LPL* breakpoint, presumably because the first base of *PEX5* exon 2 was absent (Figure 4B). The sequence of the cryptic splice acceptor site used in intron 3–4 was very similar to the splice acceptor consensus sequence and included the essential AG immediately upstream (Supplementary Figure S1A; Lodish *et al*, 2003). This splicing event resulted in a frameshift in the *PEX5* coding sequence, causing a premature stop codon (Supplementary Figure S1A). Accordingly, the *LPL–PEX5* fusion transcript could only be translated into a truncated chimeric protein.

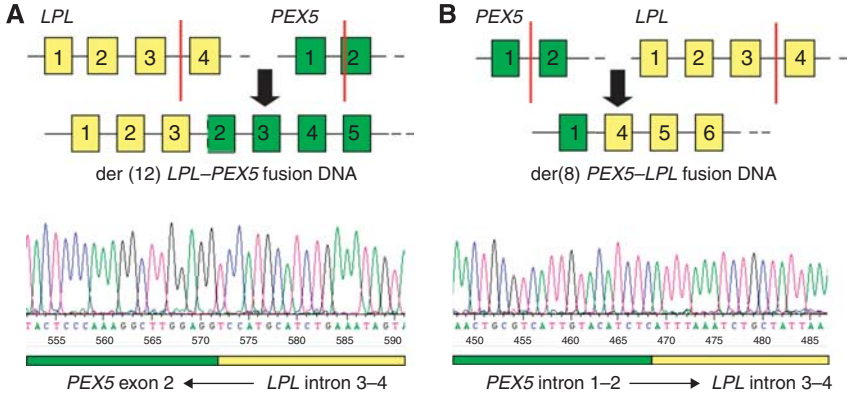

Figure 3 Schematic of breakpoints resulting in *LPL-PEX5* and *PEX5-LPL* fusion genes. Numbered boxes represent exons of *LPL* (yellow) and *PEX5* (green), with red vertical lines indicating the positions of the breakpoints resulting in the *LPL-PEX5* (**A**) and *PEX5-LPL* (**B**) fusion genes. The lower panels show the sequencing traces for each breakpoint; a reverse read in (**A**) and a forward read in (**B**).

Sequencing the *PEX5–LPL* expression PCR products identified two alternative transcripts. For the most abundant transcript (Figure 4A), there was splicing from the 3′-end of *PEX5* exon 1 into the 5′-end of *LPL* exon 4. The resulting fusion mRNA consisted of the first exon of *PEX5* followed by exons 4–10 of *LPL*, enabling translation of a full-length chimeric protein (Figure 4C). In the alternative transcript (referred to hereafter as *PEX5–LPLvar*), splicing was from within the *PEX5* intron 1–2 into *LPL* exon 4. The transcript retained the *LPL* reading frame, and therefore, could also encode a full-length chimeric protein (Figure 4C). Such alternative splicing from *PEX5* intron 1–2 has previously been documented for the wild-type transcript (http://www.ensembl.org/Homo_sapiens/Gene/Summary?g=ENSG00000139197;r=12:7341281-7371170; Supplementary Figure S1B).

We next used RT–PCR to determine the frequency of expression of wild-type *PEX5* and *LPL* in a panel of normal cervix tissue samples ($n=5$) and cervical SCC cell lines ($n=10$; Supplementary Figure S2). The *PEX5* gene was expressed ubiquitously, consistent with the function of its protein product as a peroxisome receptor (Platta and Erdmann, 2007). In contrast, *LPL* was expressed at negligible levels, in keeping with its reported tissue-specific distribution in heart, muscle and adipose tissue (Mead *et al*, 2002). In accordance with the constitutive activity of the *PEX5* promoter, the expression of *PEX5–LPL* in MS751 was significantly higher than that of *LPL–PEX5* (Figure 4D). Quantitative RT–PCR showed that *LPL* exons downstream of the breakpoint (and therefore downstream of the *PEX5* promoter) were expressed at approximately 100-fold greater abundance than those upstream of the breakpoint (and therefore downstream of the *LPL* promoter). Available antibodies against LPL were not adequate for western blot detection of the PEX5–LPL fusion protein (data not shown).

LPL is occasionally rearranged and commonly overexpressed in cervical SCCs

We tested whether *LPL* was rearranged and/or overexpressed in cervical SCC tissue samples. We performed BAC FISH on a TMA of 151 separate cervical SCCs, using differentially labelled pools of BACs mapping upstream and downstream of *LPL* (Figure 5A). Probe splitting was seen in one case, indicating that *LPL* rearrangements do occur *in vivo*, albeit rarely. In contrast, qRT–PCR showed that wild-type *LPL* was overexpressed in 10 of 28 cervical SCCs, when compared with 5 cases of normal cervix (Figure 5B). These data suggested that the same functional consequences may have resulted from translocation of *LPL* or overexpression of wild-type *LPL*. If so, the phenotypic effects of *PEX5–LPL* and full-length *LPL* in cervical SCC cells were predicted to be similar.

Overexpression of *LPL* or *PEX5–LPL* increased invasiveness of cervical SCC cells

We determined the phenotypic consequences of overexpression of *PEX5–LPL*, *PEX5–LPLvar* and full-length *LPL* in SW756, a cervical SCC cell line with negligible native *LPL* expression (Supplementary Figure S2, Figure 6A). For all three transgenes, overexpression had no effect on cell proliferation (Figure 6B), but did increase invasiveness through basement membrane extract (Figure 6C). The greatest effect was seen with overexpression of *LPL* ($P<0.0001$), but both *PEX5–LPL* and *PEX5–LPLvar* also produced a significant increase in invasion ($P<0.002$). Interestingly, the effect on invasiveness reflected the level of overexpression achieved, suggesting that each protein had a similar functional effect on cell invasiveness.

LPL overexpression also increased invasiveness in C33A, an independent second cervical SCC cell line with negligible levels of native *LPL* expression (Supplementary Figure S2, Figure 6D). The increase in cellular invasiveness was more modest relative to untreated control cells, but still significant ($P<0.009$; Figure 6E) and was not associated with increased proliferation (Figure 6F).

DISCUSSION

Improved techniques for genome analysis have indicated that reciprocal chromosomal translocations are common in solid tumours (Roschke *et al*, 2003; Kumar-Sinha *et al*, 2006). To our knowledge, ours is the first evidence of an expressed fusion gene in cervical carcinoma. Selection of the t(8;12)(p21;p13) rearrangement in MS751 is attributable to the *PEX5–LPL* fusion gene on the der(8) chromosome. The gene encoded a full-length chimeric protein and was expressed at substantially higher levels than *LPL–PEX5*, which encoded a truncated protein. These observations were in keeping with relevant gene promoter activities in cervical squamous cells, with *PEX5* being transcribed ubiquitously, but *LPL* being expressed at negligible levels. It is likely that der(12) was retained in MS751 cells to prevent loss of essential chromosomal material.

Following initial identification, the significance of any particular fusion gene can only be estimated by determining the overall prevalence *in vivo* of abnormalities involving one or the other partner gene – such as the fusion gene itself, other structural rearrangements or aberrant expression of the wild-type gene(s). In our TMA BAC FISH study, we observed *LPL* rearrangement in 1 of 151 cervical SCCs. This is in keeping with other solid tumour gene fusions, with the *ELM4–ALK* fusion being observed in as few as 2.7% of cases of non-small cell lung cancers (Perner *et al*, 2008). In addition, we may have underestimated the frequency of *LPL*

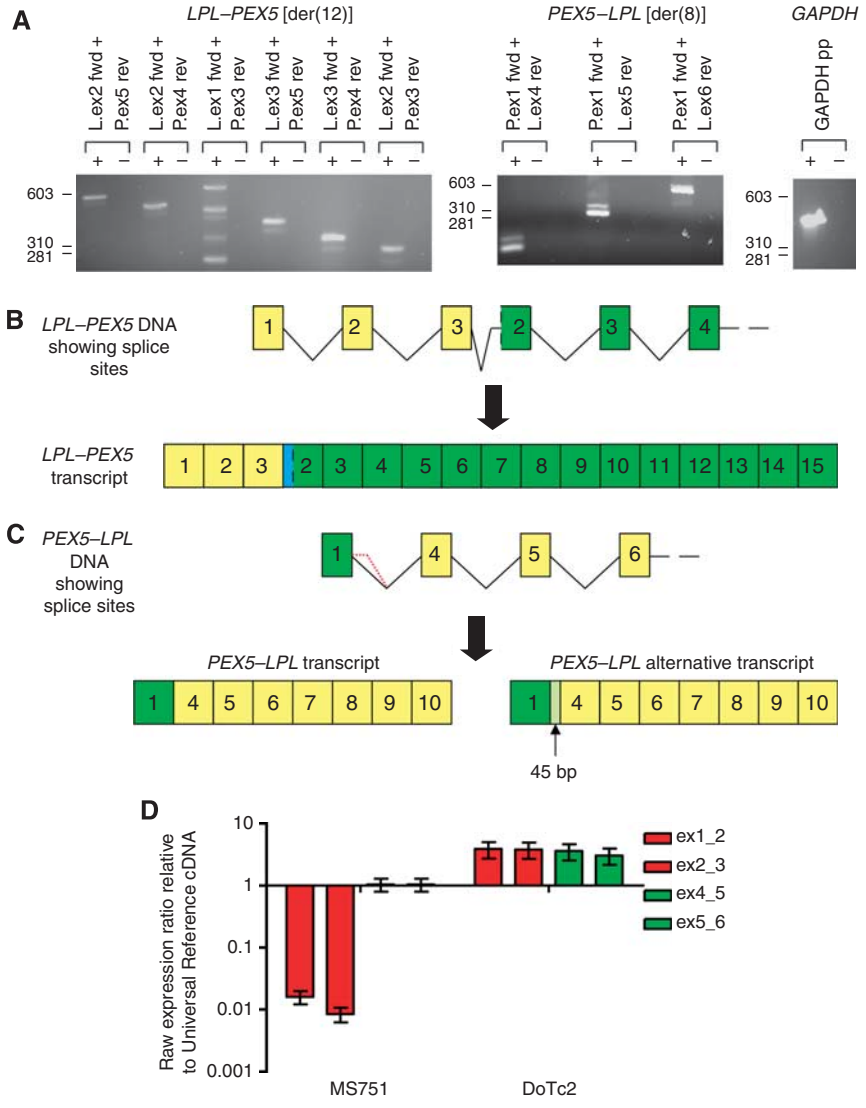

Figure 4 Identification of *LPL–PEX5* and *PEX5–LPL* transcripts in MS751. (**A**) MS751 mRNA was reverse transcribed (in the presence (+) or absence (−) of reverse transcriptase), and the cDNA amplified using primer pairs specific to exons of *LPL* (L) or *PEX5* (P). The combinations selected were specific for *LPL–PEX5* (left panel), *PEX5–LPL* (middle panel) or *GAPDH* (right panel). All primer combinations gave products, indicating that all transcripts were present in MS751 cDNA. (**B**) Sequencing PCR products showed that the *LPL–PEX5* transcript was composed of the first 3 exons of *LPL*, followed by intronic sequence of intron 3–4 of *LPL* and then exon 2 of *PEX5* without the first base, through to coding exon 15 of *PEX5*. (**C**) The most common *PEX5–LPL* transcript was composed of the first exon of *PEX5*, followed by exons 4–10 of *LPL*. Alternative splicing extended *PEX5* exon 1 into *PEX5* intron 1–2. (**D**) Quantitative RT–PCR was used to measure expression of *LPL* exons upstream and downstream of the MS751 translocation breakpoint. Ratios were referenced to Universal Reference cDNA, which was generated from a mixture of cells, including those with high *LPL* expression. Levels of upstream exons (boundaries of exons 1/2 and 2/3 (ex1_2 and ex3_4, respectively)) are in red, whereas downstream exons (boundaries of exon 4/5 and 5/6 (ex4_5 and ex5_6, respectively)) are in green. Error bars indicate the s.e.m., using four different housekeeping genes for normalisation. In MS751, downstream exons were expressed at approximately 100-fold greater abundance than upstream exons. In contrast, in the cervical SCC cell line DoTc2, which overexpressed wild-type *LPL*, there was no difference in levels of expression of upstream and downstream exons.

rearrangements *in vivo*, as the resolution of TMA BAC FISH is not sufficient to detect very small rearrangements. Given the high prevalence of cervical SCC worldwide, low frequency gene rearrangements will still contribute to substantial numbers of cases overall.

Importantly, following our identification of the *PEX5–LPL* gene fusion, we showed that wild-type *LPL* was overexpressed in around a third of cervical SCCs, relative to normal cervix. Regulation of *LPL* expression is complex, involving both transcriptional and post-transcriptional processes (Mead *et al*, 2002), and the mechanism of full-length *LPL* overexpression in cervical SCC remains to be determined. Such frequent *LPL* overexpression *in vivo* further supported the evidence that the selective advantage provided by the reciprocal translocation in MS751 was due to overexpression of functional exons of *LPL*. If so, wild-type LPL and the PEX5–LPL fusion protein would be predicted to have similar functional roles in cervical SCC.

Although the best-described function of LPL is hydrolysis of triacylglycerol (triglyceride) and generation of fatty acids (Mead *et al*, 2002), *PEX5–LPL* and *PEX5–LPLvar* are missing the first three exons of *LPL*, and therefore, parts of the N-terminal domain of the wild-type protein that are essential for such catalytic function (Semenkovich *et al*, 1990; Ben-Zeev *et al*, 1994). In general agreement with this observation, overexpression of *LPL* or the fusion genes in cervical SCC cells did not increase cell growth, which is a common consequence of increased cellular metabolic activity (Jones and Thompson, 2009). In contrast, overexpression of all three transgenes did increase cellular invasion to an extent

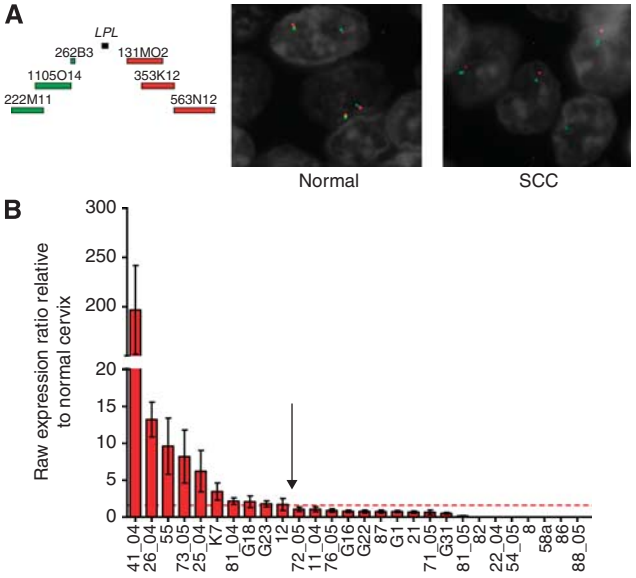

Figure 5 *LPL* status in cervical SCC. (**A**) For TMA FISH, the probes were three tiling BACs 5′ of *LPL* and three tiling BACs 3′ of *LPL*, which were labelled in green and red, respectively (left panel). The DNA counterstain (4′,6-diamidino-2-phenylindole) is shown in grey. Co-localisation of probes was seen in normal cervix samples (middle panel) and 150/151 primary cervical SCC samples. One cervical SCC sample showed probe separation (right panel), indicating rearrangement of the *LPL* gene. Interestingly, this case also showed deletion of the wild-type *LPL* allele. (**B**) Quantitative RT–PCR to measure levels of full-length *LPL* was performed on 28 cervical SCC samples and 5 normal cervical squamous epithelium samples, relative to Universal Reference cDNA. Error bars indicate the s.e.m. for *LPL* expression levels, normalised to four different housekeeping genes. The dashed line shows 3 standard deviations above the mean of the five normal samples. Ten tissue samples (left of arrow) showed a significantly higher level of *LPL* expression than normal cervix.

equivalent to transcript abundance. We conclude that the LPL domain that provided a selective advantage in cervical SCC cells was likely to be shared between the three transgenes, and accordingly, was most likely to be in the C-terminal region, which is essential for many of the non-catalytic functions of LPL. Interestingly, recurrent overexpression of *LPL* has also been observed in chronic lymphocytic leukaemia (CLL), where it is an adverse prognostic marker (Heintel *et al*, 2005; Oppezzo *et al*, 2005). In keeping with our data, overexpressed LPL in CLL is not associated with increased catalytic activity (Mansouri *et al*, 2010).

After synthesis in parenchymal cells, LPL passes through the endoplasmic reticulum and is secreted. It binds heparan sulphate proteoglycans (HSPG; Braun and Severson, 1992) and is translocated to HSPG-binding sites on the luminal surface of the capillary epithelium, potentially along a bridge of HSPGs in the extracellular matrix (Blanchette-Mackie *et al*, 1989). Non-catalytic functions of LPL include dimerisation and bridging between lipoproteins and cell surface receptors such as HSPG (Merkel *et al*, 1998). Bridging may involve different cell types, requiring LPL dimerisation and HSPG on both surfaces (Mamputu *et al*, 1997; Obunike *et al*, 1997). Accordingly, expression of LPL by malignant cells may promote tumorigenesis by enabling the cell–stromal interactions that are critical for tumour maintenance (Mansouri *et al*, 2010).

Importantly, HSPGs are abundant in the extracellular matrix (ECM) of various malignancies, including carcinomas (Iozzo *et al*, 1994). Elevated expression of HSPGs has been associated with increased metastasis and it has been proposed that HSPGs in the ECM form an adhesive tract for cell migration (Sanderson, 2001). Our data support a model in which LPL, PEX5–LPL or PEX5–LPLvar, all sharing the non-catalytic LPL C terminus, bridge between HSPGs on the cell surface and in the ECM, thereby promoting cell invasion (Supplementary Figure S3). The PEX5–LPL and PEX5–LPLvar fusion proteins do not possess the N-terminal signal peptide responsible for targeting LPL to the endoplasmic reticulum before secretion, and are therefore unlikely to be processed in the same manner as full-length LPL. Interestingly, the first exon of PEX5 might

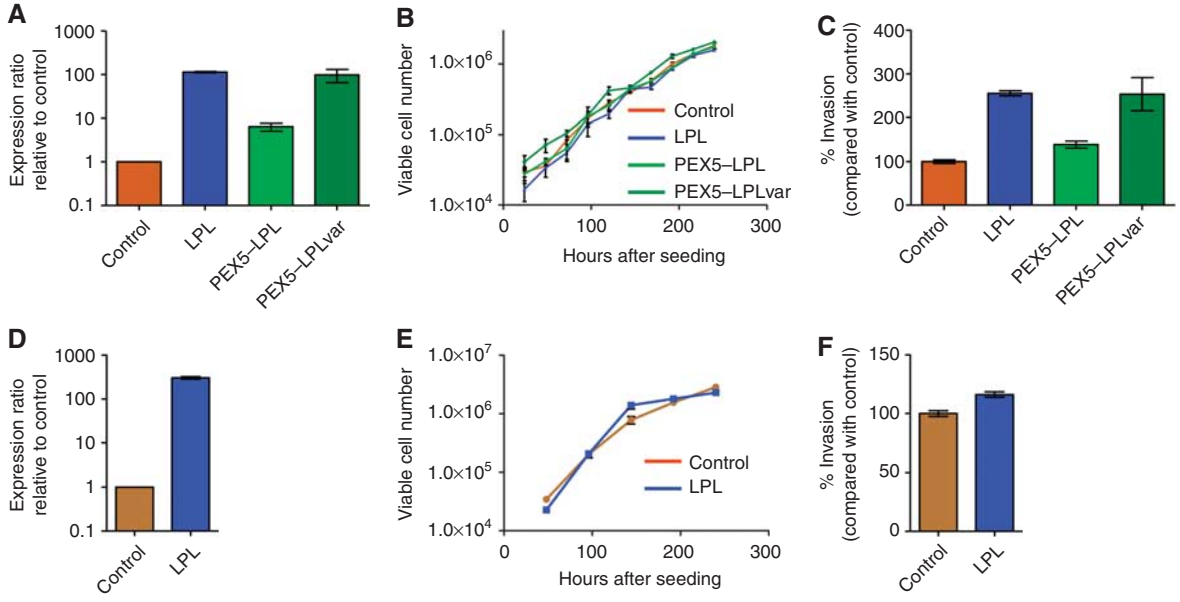

Figure 6 Phenotypic consequences of overexpression of wild-type LPL or LPL fusion proteins in cervical SCC cells. The top row (**A**–**C**) shows the effects of overexpressing wild-type LPL and the PEX5–LPL fusion proteins in SW756 cells, whereas the bottom row (**D**–**F**) shows the effects of overexpressing wild-type LPL in C33A cells. (**A**, **D**) Expression levels were determined by qRT–PCR, using primers for the C terminus of *LPL*, which was present in all transgenes. (**B**, **E**) Growth curves were generated for stable populations of cells expressing PEX5–LPL, PEX5–LPLvar or LPL, compared with those transfected with empty vector. Error bars indicate the s.e.m. between triplicate wells. There were no significant differences in growth. (**C**, **F**) Invasion through basement membrane extract was measured and expressed as the percentage of invading cells relative to control. Error bars indicate the s.e.m. between triplicate assays. Wild-type LPL and the fusion proteins consistently increased the invasiveness of cervical SCC cells.

contribute to secretion of the fusion protein, as PEX5 is known to have intrinsic lipid-binding activity (Kerssen *et al*, 2006). This is an attractive and testable model, and indicates the need for further work to determine how LPL, PEX5–LPL and PEX5–LPLvar contribute to cervical SCC cell invasiveness.

We conclude that *LPL* is frequently deregulated in cervical SCC, either because of overexpression of the wild-type gene or, more rarely, because of translocation, as exemplified by the *PEX5–LPL* gene fusion that we identified in MS751. The selective advantage is provided by the non-catalytic C-terminal domain, which increases the invasiveness of cervical SCC cells. The functional interactions of this domain may represent a novel therapeutic target in cervical SCC and potentially other tumour types.

ACKNOWLEDGEMENTS

We thank Dr Suet-Feung Chin for help with interpreting interphase FISH data and Ms Konstantina Karagavriilidou for providing tissue sample RNA. This study was supported by Cancer Research UK and the Medical Research Council.

Conflict of interest

The authors declare no conflict of interest.

Supplementary Information accompanies the paper on British Journal of Cancer website (http://www.nature.com/bjc)

REFERENCES

Arends MJ, Buckley CH, Wells M (1998) Aetiology, pathogenesis, and pathology of cervical neoplasia. *J Clin Pathol* **51**(2): 96–103

Baldwin P, Laskey R, Coleman N (2003) Translational approaches to improving cervical screening. *Nat Rev Cancer* **3**(3): 217–226

Ben-Zeev O, Stahnke G, Liu G, Davis RC, Doolittle MH (1994) Lipoprotein lipase and hepatic lipase: the role of asparagine-linked glycosylation in the expression of a functional enzyme. *J Lipid Res* **35**(9): 1511–1523

Blanchette-Mackie EJ, Masuno H, Dwyer NK, Olivecrona T, Scow RO (1989) Lipoprotein lipase in myocytes and capillary endothelium of heart: immunocytochemical study. *Am J Physiol* **256**(6 Part 1): E818–E828

Bosch FX, Manos MM, Munoz N, Sherman M, Jansen AM, Peto J, Schiffman MH, Moreno V, Kurman R, Shah KV (1995) Prevalence of human papillomavirus in cervical cancer: a worldwide perspective. International biological study on cervical cancer (IBSCC) Study Group. *J Natl Cancer Inst* **87**(11): 796–802

Braun JE, Severson DL (1992) Regulation of the synthesis, processing and translocation of lipoprotein lipase. *Biochem J* **287**(Part 2): 337–347

Dowen SE, Neutze DM, Pett MR, Cottage A, Stern P, Coleman N, Stanley MA (2003) Amplification of chromosome 5p correlates with increased expression of Skp2 in HPV-immortalized keratinocytes. *Oncogene* **22**(16): 2531–2540

Edwards PA (2010) Fusion genes and chromosome translocations in the common epithelial cancers. *J Pathol* **220**(2): 244–254

Foster N, Carter S, Ng G, Pett M, Roberts I, Coleman N (2009) Molecular cytogenetic analysis of cervical squamous cell carcinoma cells demonstrates discordant levels of numerical and structural chromosomal instability and identifies 'selected' chromosome rearrangements. *Cytogenet Genome Res* **127**(1): 9–20

Ganem NJ, Storchova Z, Pellman D (2007) Tetraploidy, aneuploidy and cancer. *Curr Opin Genet Dev* **17**(2): 157–162

Harris CP, Lu XY, Narayan G, Singh B, Murty VV, Rao PH (2003) Comprehensive molecular cytogenetic characterization of cervical cancer cell lines. *Genes Chromosomes Cancer* **36**(3): 233–241

Heintel D, Kienle D, Shehata M, Krober A, Kroemer E, Schwarzinger I, Mitteregger D, Le T, Gleiss A, Mannhalter C, Chott A, Schwarzmeier J, Fonatsch C, Gaiger A, Dohner H, Stilgenbauer S, Jager U (2005) High expression of lipoprotein lipase in poor risk B-cell chronic lymphocytic leukemia. *Leukemia* **19**(7): 1216–1223

Heselmeyer K, Schrock E, du Manoir S, Blegen H, Shah K, Steinbeck R, Auer G, Ried T (1996) Gain of chromosome 3q defines the transition from severe dysplasia to invasive carcinoma of the uterine cervix. *Proc Natl Acad Sci USA* **93**(1): 479–484

Hidalgo A, Baudis M, Petersen I, Arreola H, Pina P, Vazquez-Ortiz G, Hernandez D, Gonzalez J, Lazos M, Lopez R, Perez C, Garcia J, Vazquez K, Alatorre B, Salcedo M (2005) Microarray comparative genomic hybridization detection of chromosomal imbalances in uterine cervix carcinoma. *BMC Cancer* **5**: 77

Holowaty P, Miller AB, Rohan T, To T (1999) Natural history of dysplasia of the uterine cervix. *J Natl Cancer Inst* **91**(3): 252–258

Iozzo RV, Cohen IR, Grassel S, Murdoch AD (1994) The biology of perlecan: the multifaceted heparan sulphate proteoglycan of basement membranes and pericellular matrices. *Biochem J* **302**(Part 3): 625–639

Jones RG, Thompson CB (2009) Tumor suppressors and cell metabolism: a recipe for cancer growth. *Genes Dev* **23**(5): 537–548

Kerssen D, Hambruch E, Klaas W, Platta HW, de Kruijff B, Erdmann R, Kunau WH, Schliebs W (2006) Membrane association of the cycling peroxisome import receptor Pex5p. *J Biol Chem* **281**(37): 27003–27015

Kumar-Sinha C, Tomlins SA, Chinnaiyan AM (2006) Evidence of recurrent gene fusions in common epithelial tumors. *Trends Mol Med* **12**(11): 529–536

Lockwood WW, Coe BP, Williams AC, MacAulay C, Lam WL (2007) Whole genome tiling path array CGH analysis of segmental copy number alterations in cervical cancer cell lines. *Int J Cancer* **120**(2): 436–443

Lodish H, Berk A, Zipursky S, Matsudaira P, Baltimore D, Darnell J, Zipursky L (2003) *Molecular Cell Biology*. W.H. Freeman & Co Limited: New York, NY, USA

Mamputu JC, Desfaits AC, Renier G (1997) Lipoprotein lipase enhances human monocyte adhesion to aortic endothelial cells. *J Lipid Res* **38**(9): 1722–1729

Mansouri M, Sevov M, Fahlgren E, Tobin G, Jondal M, Osorio L, Roos G, Olivecrona G, Rosenquist R (2010) Lipoprotein lipase is differentially expressed in prognostic subsets of chronic lymphocytic leukemia but displays invariably low catalytical activity. *Leuk Res* **34**(3): 301–306

Mead JR, Irvine SA, Ramji DP (2002) Lipoprotein lipase: structure, function, regulation, and role in disease. *J Mol Med* **80**(12): 753–769

Merkel M, Kako Y, Radner H, Cho IS, Ramasamy R, Brunzell JD, Goldberg IJ, Breslow JL (1998) Catalytically inactive lipoprotein lipase expression in muscle of transgenic mice increases very low density lipoprotein uptake: direct evidence that lipoprotein lipase bridging occurs *in vivo*. *Proc Natl Acad Sci USA* **95**(23): 13841–13846

Ng G, Winder D, Muralidhar B, Gooding E, Roberts I, Pett M, Mukherjee G, Huang J, Coleman N (2007) Gain and overexpression of the oncostatin M receptor occur frequently in cervical squamous cell carcinoma and are associated with adverse clinical outcome. *J Pathol* **212**(3): 325–334

Obunike JC, Paka S, Pillarisetti S, Goldberg IJ (1997) Lipoprotein lipase can function as a monocyte adhesion protein. *Arterioscler Thromb Vasc Biol* **17**(7): 1414–1420

Oppezzo P, Vasconcelos Y, Settegrana C, Jeannel D, Vuillier F, Legarff-Tavernier M, Kimura EY, Bechet S, Dumas G, Brissard M, Merle-Beral H, Yamamoto M, Dighiero G, Davi F (2005) The LPL/ADAM29 expression ratio is a novel prognosis indicator in chronic lymphocytic leukemia. *Blood* **106**(2): 650–657

Patel RM, Downs-Kelly E, Weiss SW, Folpe AL, Tubbs RR, Tuthill RJ, Goldblum JR, Skacel M (2005) Dual-color, break-apart fluorescence *in situ* hybridization for EWS gene rearrangement distinguishes clear cell sarcoma of soft tissue from malignant melanoma. *Mod Pathol* **18**(12): 1585–1590

Perner S, Wagner PL, Demichelis F, Mehra R, Lafargue CJ, Moss BJ, Arbogast S, Soltermann A, Weder W, Giordano TJ, Beer DG, Rickman DS, Chinnaiyan AM, Moch H, Rubin MA (2008) EML4-ALK fusion lung cancer: a rare acquired event. *Neoplasia* **10**(3): 298–302

Pett M, Coleman N (2007) Integration of high-risk human papillomavirus: a key event in cervical carcinogenesis? *J Pathol* **212**(4): 356–367

Pett MR, Alazawi WO, Roberts I, Dowen S, Smith DI, Stanley MA, Coleman N (2004) Acquisition of high-level chromosomal instability is associated with integration of human papillomavirus type 16 in cervical keratinocytes. *Cancer Res* **64**(4): 1359–1368

Pfaffl MW (2001) A new mathematical model for relative quantification in real-time RT-PCR. *Nucleic Acids Res* **29**(9): e45

Platta HW, Erdmann R (2007) Peroxisomal dynamics. *Trends Cell Biol* **17**(10): 474–484

Rao PH, Arias-Pulido H, Lu XY, Harris CP, Vargas H, Zhang FF, Narayan G, Schneider A, Terry MB, Murty VV (2004) Chromosomal amplifications, 3q gain and deletions of 2q33–q37 are the frequent genetic changes in cervical carcinoma. *BMC Cancer* **4**: 5

Roschke AV, Tonon G, Gehlhaus KS, McTyre N, Bussey KJ, Lababidi S, Scudiero DA, Weinstein JN, Kirsch IR (2003) Karyotypic complexity of the NCI-60 drug-screening panel. *Cancer Res* **63**(24): 8634–8647

Sanderson RD (2001) Heparan sulfate proteoglycans in invasion and metastasis. *Semin Cell Dev Biol* **12**(2): 89–98

Semenkovich CF, Luo CC, Nakanishi MK, Chen SH, Smith LC, Chan L (1990) *In vitro* expression and site-specific mutagenesis of the cloned human lipoprotein lipase gene. Potential N-linked glycosylation site asparagine 43 is important for both enzyme activity and secretion. *J Biol Chem* **265**(10): 5429–5433

Shing DC, McMullan DJ, Roberts P, Smith K, Chin SF, Nicholson J, Tillman RM, Ramani P, Cullinane C, Coleman N (2003) FUS/ERG gene fusions in Ewing's tumors. *Cancer Res* **63**(15): 4568–4576

Soda M, Choi YL, Enomoto M, Takada S, Yamashita Y, Ishikawa S, Fujiwara S, Watanabe H, Kurashina K, Hatanaka H, Bando M, Ohno S, Ishikawa Y, Aburatani H, Niki T, Sohara Y, Sugiyama Y, Mano H (2007) Identification of the transforming EML4-ALK fusion gene in non-small-cell lung cancer. *Nature* **448**(7153): 561–566

Tomlins SA, Rhodes DR, Perner S, Dhanasekaran SM, Mehra R, Sun XW, Varambally S, Cao X, Tchinda J, Kuefer R, Lee C, Montie JE, Shah RB, Pienta KJ, Rubin MA, Chinnaiyan AM (2005) Recurrent fusion of TMPRSS2 and ETS transcription factor genes in prostate cancer. *Science* **310**(5748): 644–648

Walboomers JM, Jacobs MV, Manos MM, Bosch FX, Kummer JA, Shah KV, Snijders PJ, Peto J, Meijer CJ, Munoz N (1999) Human papillomavirus is a necessary cause of invasive cervical cancer worldwide. *J Pathol* **189**(1): 12–19

zur Hausen H (2000) Papillomaviruses causing cancer: evasion from host-cell control in early events in carcinogenesis. *J Natl Cancer Inst* **92**(9): 690–698